Journal of Biomolecular Structure and Dynamics





ISSN: (Print) (Online) Journal homepage: www.tandfonline.com/journals/tbsd20

Conformational fluidity of intrinsically disordered proteins in crowded environment: a molecular dynamics simulation study

Carolyn Shult, Keegan Gunderson, Stephen J. Coffey, Brenya McNally, Michael Brandt, Lucille Smith, Joshua Steczynski, Ethan R. Olerich, Sydney E. Schroeder, Nathaniel J. Severson, Sanchita Hati & Sudeep Bhattacharyay

To cite this article: Carolyn Shult, Keegan Gunderson, Stephen J. Coffey, Brenya McNally, Michael Brandt, Lucille Smith, Joshua Steczynski, Ethan R. Olerich, Sydney E. Schroeder, Nathaniel J. Severson, Sanchita Hati & Sudeep Bhattacharyay (16 Sep 2024): Conformational fluidity of intrinsically disordered proteins in crowded environment: a molecular dynamics simulation study, Journal of Biomolecular Structure and Dynamics, DOI: 10.1080/07391102.2024.2404531

To link to this article: https://doi.org/10.1080/07391102.2024.2404531

+	View supplementary material 🗗
	Published online: 16 Sep 2024.
	Submit your article to this journal 🗷
a ^L	View related articles 🗗
CrossMark	View Crossmark data 🗹





Conformational fluidity of intrinsically disordered proteins in crowded environment: a molecular dynamics simulation study

Carolyn Shult, Keegan Gunderson, Stephen J. Coffey, Brenya McNally, Michael Brandt, Lucille Smith, Joshua Steczynski, Ethan R. Olerich, Sydney E. Schroeder, Nathaniel J. Severson, Sanchita Hati and Sudeep Bhattacharyay so

Department of Chemistry and Biochemistry, University of Wisconsin-Eau Claire, Eau Claire, WI, USA Communicated by Ramaswamy H. Sarma

ABSTRACT

The class of intrinsically disordered proteins lacks stable three-dimensional structures. Their flexibility allows them to engage in a wide variety of interactions with other biomolecules thus making them biologically relevant and efficient. The intrinsic disorders of these proteins, which undergo binding-induced folding, allow alterations in their topologies while conserving their binding sites. Due to the lack of well-defined three-dimensional structures in the absence of their physiological partners, the folding and the conformational dynamics of these proteins remained poorly understood. Particularly, it is unclear how these proteins exist in the crowded intracellular milieu. In the present study, molecular dynamic simulations of two intrinsically unstructured proteins and two controls (folded proteins) were conducted in the presence and absence of molecular crowders to obtain an in-depth insight into their conformational flexibility. The present study revealed that polymer crowders stabilize the disordered proteins through enthalpic as well as entropic effects that are significantly more than their monomeric counterpart. Taken together, the study delves deep into crowding effects on intrinsically disordered proteins and provides insights into how molecular crowders induce a significantly diverse ensemble of dynamic scaffolds needed to carry out diverse functions.

Abbreviations: CDK1P: cyclin-dependent kinase inhibitor 1-interacting protein; IDP: intrinsically disordered protein; MD: molecular dynamics; PEG: polyethylene glycol; PCA: principal component analysis; RMSD: root-mean-square deviation; XPA: Xeroderma Pigmentosum group A

ARTICLE HISTORY

Received 23 January 2024 Accepted 8 April 2024

KEYWORDS

Intrinsically dynamic proteins; intrinsically flexible proteins; intrinsically disordered proteins; molecular crowding; molecular dynamic simulation

1. Introduction

Intrinsically disordered proteins (IDPs), also known as intrinsically dynamic or unstructured proteins, lack stable secondary or tertiary structures. Due to their lack of stable structure, IDPs are very flexible. The disordered nature of these proteins allows them to have the potential to bind to a variety of biological partners. They interact with biomolecules such as DNA, RNA, proteins and carbohydrates (Bonucci et al., 2021; Uversky, 2009) and play essential roles in cell proliferation, cell signaling and protein-protein interactions and facilitate molecular communications (Bondos et al., 2022; Dunker et al., 2002; Dyson & Wright, 2005; Morris et al., 2021; Wright & Dyson, 1999).

Proteins are fundamental for the existence of all living organisms, yet the process of protein folding remains largely a mystery (Gething & Sambrook, 1992; Uversky, 2019). The complete structure of these workhorses of life is described at four levels: primary, secondary, tertiary and quaternary. The primary structure is the linear amino acid sequence, the secondary structure is the local spatial arrangement of the

protein backbone, and the tertiary and quaternary structures are the three-dimensional organization adopted by a single polypeptide chain and multiple subunits, respectively, as they interact with the aqueous milieu (Rehman et al., 2022). The protein folding problem remains a challenging problem and it is the question of how a protein's primary structure dictates its unique three-dimensional structure and what is the overall folding mechanism (Dill et al., 2008; Gething & Sambrook, 1992). The complex three-dimensional architecture of a protein and its stability are attributed to the combined effect of various noncovalent interactions. The tertiary/quaternary structure of a protein governs its function. Thus, the influence of the aqueous environment on the structure and its consequences on protein function is crucial to understand, as changes within the surrounding environment can profoundly impact a protein's structure and consequently, its function. For instance, numerous studies have shown that macromolecular crowding can influence various aspects of protein properties, including protein fibrillation, folding rates, native structure stability, binding interactions, nuclear body formation and macromolecular transport (Cheung et al., 2005; Cho & Kim, 2012; Fagerberg et al., 2019; Fonin et al., 2018; Menon & Mondal, 2023; Munishkina et al., 2008; Qi et al., 2014; Zhou, 2008; Zhou et al., 2008).

Due to their flexibility and lack of defined structure, IDPs are notoriously difficult to study using conventional techniques, such as X-ray crystallography (Li et al., 2018; Na et al., 2018). To gain insight into the structure of IDPs without the need for crystallization, alternative methods such as Small-Angle X-ray Scattering (SAXS) and Nuclear Magnetic Resonance (NMR) spectroscopy are used. NMR spectroscopy, leveraging the magnetic properties of atomic nuclei, has proved helpful in determining the three-dimensional conformations of IDPs (Dyson & Wright, 2004; Felli & Pierattelli, 2012; Kosol et al., 2013). SAXS, on the other hand, is a useful tool for studying the shape, flexibility and conformational polydispersity of IDPs (Fagerberg et al., 2019; Kikhney & Svergun, 2015; Receveur-Brechot & Durand, 2012). While these techniques are powerful, they are more informative when combined with additional experimental or molecular simulation data (Evans et al., 2023; Putnam et al., 2007). The development of computational methods like AlphaFold, an artificial intelligence method developed by DeepMind (Bertoline et al., 2023; Jumper et al., 2021; Straiton, 2023; Varadi et al., 2022) for predicting protein structure and folding patterns (Jumper et al., 2021; Varadi et al., 2022), has aided in gaining a more comprehensive understanding of IDPs (Bertoline et al., 2023; Jumper et al., 2021; Straiton, 2023); computational methods helped to overcome challenges associated with studying IDPs using traditional experimental techniques (Chong et al., 2017; Li et al., 2018). An understanding of the folding and dynamics of the IDPs within the intracellular space can have a range of benefits. IDPs in the intracellular space are known to exhibit liquidliquid phase separation behavior (Dignon et al., 2019; Dzuricky et al., 2020; Lin & Chan, 2017; Quiroz et al., 2019), a knowledge of which has the potential for designing biomaterials and drug delivery (Dignon et al., 2019). Furthermore, it has been observed that within the intracellular milieu, other biomolecules influence protein folding and conformational space through crowding and confinement (Fonin et al., 2018; Sarkar et al., 2022; Zimmerman & Minton, 1993). Due to the ability of IDPs to adapt many different structures according to the changes in intracellular conditions, they are especially susceptible to the influence of crowders in their environments (Fagerberg et al., 2019; Fonin et al., 2018; Menon &

Mondal, 2023; Soranno et al., 2014; Uversky, 2009). Currently, there is a lack of information regarding the conformations of these disordered proteins in intracellular environments. We hypothesize that interactions with crowders will lead to a change in the conformational space and folding landscape of IDPs, a process that could likely alter their functions. The change in folding pattern can be studied by following conformational dynamics and shifts in the conformational ensemble for each IDP. Thus, in the present study, we studied the conformational changes of two disordered proteins and two folded proteins as controls in crowded environments using molecular dynamics (MD) simulations. The functions of these four proteins, which are about similar size, with varying degrees of disorders are briefly described in Table 1. Briefly, GTPase HRas, without the C-terminus, is a well-folded enzyme (Figure 1(a)) with critical roles in cell signaling, including regulation of the cell cycle via cyclindependent kinases, cell differentiation and apoptosis. Mutations of GTPase HRas proteins are linked to many cancer types, including bladder and thyroid cancers (Berrada et al., 2015; Garcia-Rostan et al., 2003; Malumbres & Barbacid, 2003; Nikiforov & Nikiforova, 2011; Vageli et al., 1996). The second protein studied was Xeroderma Pigmentosum group A (XPA), which is an IDP and involved in DNA repair pathways by regulating nucleotide excision repair (NER) pathways (Rademakers et al., 2003; Sugasawa et al., 1998). Mutations in the XPA protein may lead to extreme sensitivity to UV light, as the ability to rectify DNA damage is impaired (Bradford et al., 2011; García-Carmona et al., 2021; Vries et al., 1995). This IDP has significantly unfolded regions (Figure 1(b)) and is therefore predicted to exhibit larger changes in conformation in crowded environments.

Cyclin-dependent kinase inhibitor 1-interacting protein (CDK1P) is another IDP, which mediates the G1-to-S phase transition of the cell cycle. The G1 checkpoint is responsible for controlling cell growth and division and is regulated by cyclin-dependent kinases (CDK). CDK1P inhibits these CDKs, causing cells to arrest in G1 (Al Bitar & Gali-Muhtasib, 2019; Bertoli et al., 2013; Deng et al., 1995). The native structure of this protein is primarily unfolded (Figure 1(c)) and is therefore predicted to experience greater conformational changes in vivo (Kriwacki et al., 1996). Lastly, the von Hippel-Lindau tumor suppressor protein (pVHL) plays an essential role in cellular oxygen sensing, targeting hypoxia-inducible factors for ubiquitination and degradation. Mutations of the pVHL

Table 1. Summary of proteins utilized throughout simulations, including abbreviations and core functions.

Protein full name	Abbreviated name	Core function
GTPase HRas	GTPase HRas	GTPase activity ie GTP/GDP binding and hydrolysis. https://www.ncbi.nlm.nih.gov/gene/3265
Xeroderma Pigmentosum group A	ХРА	Zinc finger protein is involved in repairing DNA damage via nucleotide excision repair. https://www.ncbi.nlm. nih.gov/gene/7507
Cyclin-dependent kinase inhibitor 1-interacting protein	CDK1P	Regulator of cell cycle progression at G1; binds to and inhibits the activity of cyclin-dependent kinases (2 and 4). https://www.ncbi.nlm.nih.gov/gene/1026
von Hippel-Lindau tumor suppressor protein	pVHL	Encodes component of ubiquitination complex; involved in ubiquitination and oxygen-related gene expression (<i>via</i> degradation of hypoxia-inducible factor). https://www.ncbi.nlm.nih.gov/gene/7428

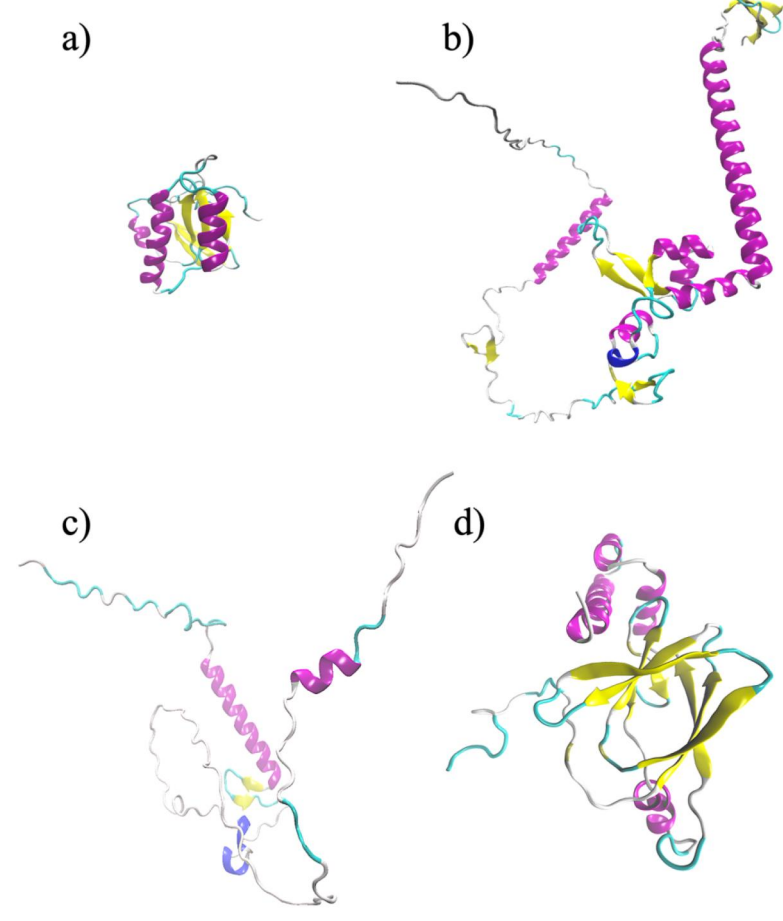


Figure 1. The alpha-fold generated structure of the four proteins studied (a) GTPase HRas, (b) XPA, (c) CDK1P and (d) pVHL.

protein are associated with tumorigenesis or Von Hippel-Lindau disease, characterized by highly vascularized tumors in vital human organs such as the spinal cord, retina and blood vessels in the brain (Igarashi et al., 2002; Kaelin, 2002, 2007; Kim & Kaelin, 2004; Ohh et al., 2022). This protein is partially folded (Figure 1(d)) and therefore is expected to undergo limited conformational changes within the intracellular space.

The focus of the present study was to elucidate how the conformational dynamics of IDPs and folded proteins (controls) respond to the changes in the crowded intracellular milieu. The crowded environment was generated by exposing these four target proteins to commonly used synthetic crowders, ethylene glycol (abbreviated hereafter as EG) and its polymers, polyethylene glycols (PEG, $C_{2n}H_{4n+2}O_{n+1}$), of varying molecular weights. Using 50 ns MD simulations and subsequent conformational analyses, we probed how crowders impacted the conformational landscape of the proteins under consideration.

2. Methods

The conformational dynamics of the above-mentioned four proteins (two IDPs and two controls) were analyzed in the presence of synthetic crowders. For these proteins, structural coordinates were obtained from the AlphaFold Protein Structure Database (Jumper et al., 2021). AlphaFold uses DeepMind to help predict the 3-D structure of a protein based

on the primary amino acid sequence (Jumper et al., 2021; Varadi et al., 2022). The proteins were then visualized using Visual Molecular Dynamics (VMD) (Humphrey et al., 1996), a 3-D molecular visualization program that can animate large biomolecular systems. All simulations were performed using GPU-enabled Nanoscale Molecular Dynamics (NAMD) (Phillips et al., 2020) using CHARMM36 force field (Brooks et al., 1983; Huang & Mackerell, 2013). Computations were carried out on the hybrid GPU-CPU Cluster (containing a total of 61 nodes and 3904 cores) at the Blugold Center for High-Performance Computing, UW-Eau Claire. MD simulations were carried out using the NAMD program (Phillips et al., 2005, 2020) on GPU nodes, each equipped with NVIDIA Tesla V100S 32GB GPU cards. Five different systems were built for each protein in (i) only water, (ii) crowded with EG and (iii)-(v) crowded with varying-sized PEG crowders (molecular weights \sim 600, 8k and 20k Da). Lastly, 50 ns MD simulations were performed, and dcd trajectory files were used for further analysis of each system. The effects of molecular crowding on conformational dynamics and energetics were studied in detail using statistical tools.

2.1. Building up of crowder-protein-solvent systems

Hydrogen atoms were added to the protein structures by using standard scripts of VMD (Humphrey et al., 1996). PEG molecules were built as described previously (Laatsch

et al., 2023). Using scripts generated in our lab, crowders were added and distributed around the target proteins. These crowders included EG, PEG 600, PEG 8k and PEG 20k. For PEG 8k and PEG 20k systems, these molecules were first simulated in water for 2 ns before being placed around the target protein, within the van der Waals interaction range. Each target protein in the crowded environment was then solvated in a water box so that all water molecules within 2.4 Å distance from the protein atoms were eliminated (Jorgensen et al., 1983). To minimize the solvent volume, the protein-crowder complex was rotated in 10 increments and a 25 Å padding was maintained in all three dimensions. The solvated system was neutralized with ions.

2.2. Minimization and dynamics

Following the creation of the water box and ionization of the protein system, two separate minimizations were performed. The first consisted of 5000 steps in which the backbone remained fixed. The second minimization utilized 20,000 steps in which case all atoms moved freely, including the previously fixed protein backbone. This was followed by MD simulations of 50 ns using NAMD implementation of Langevin dynamics under periodic boundary conditions (Cheatham et al., 1995). Non-bonding interactions were modeled using a switching function with a 'switchdist' of 10 Å, a cutoff of 14 Å and a 'pairlistdist' of 16 Å. Electrostatic interactions were evaluated using the particle mesh Ewald method (Essmann et al., 1995). A time step of 2-fs was used in the leapfrog Verlet algorithm for integration (Verlet, 1967). For conformational sampling, a constant pressure dynamics was run generating isothermal-isobaric (NPT) ensemble (Feller et al., 1995) which provided the enthalpic changes of the molecular systems.

2.3. Essential dynamics analysis

The MD simulation trajectories were analyzed by studying the principal component of motions (Amadei et al., 1993; Tan et al., 2014), which is also known as essential dynamics analysis (EDA). The analysis produces the largest variance of the data, which in the present case would represent the collectivity of backbone motion.

The root-mean-square deviation per frame, the principal components and per-residue fluctuations were determined using the program CARMA (Glykos, 2006). The root-mean-square deviation (RMSD) for the *i*th frame is calculated from the square root of the mean square of the deviations, averaging the overall C_{α} atoms for that specific frame using Equation (1).

RMSD =
$$\sqrt{\frac{1}{N} \sum_{j=1}^{N} (r_{i,j} - r_{0,j})^2}$$
 (1)

The calculation for root-mean-square deviation, where N is the number of C_{α} atoms, and $r_{i,j}$ and $r_{0,j}$ are position vectors for the jth C_{α} atom observed in the ith frame and the 0^{th} (ie starting frame), respectively. The principal

components were generated using the $C_{\alpha}-C_{\alpha}$ covariance matrix using the entire 50 ns trajectory data. Analysis of the conformational ensemble was carried out using the top two clusters selected based on contributions of the first three principal components of motion (Glykos, 2006). Molecular structures corresponding to two densely populated clusters were used for further visual analysis and for generating average representative structures for each cluster. The RMSD of these average structures, calculated using Equation (1), represented the extent of conformational diversity of the protein, produced under the constraints of each crowding environment.

2.4. Calculation of energetics

The energetic changes were computed from the stored conformations of 50 ns MD simulations. The enthalpic changes for the solvated protein-crowder system were calculated from the total energy values averaging over 0.2 ns. In addition to the total energy changes, the crowder-protein interaction energies were also computed. To study the entropy of the protein component of the system only, Schlitter's configurational entropy was computed (Schlitter, 1993).

3. Results and discussions

In the study, two significantly disordered (XPA and CDK1P) and two well-folded (GTPase HRas and pVHL) protein systems were studied in four different crowding conditions and compared with the dilute condition. These proteins were of small size (<5000 atoms) as illustrated in Table S1. The assemblies of these solvated protein-crowder systems were of varied dimensions and atom sizes (Table S1). Two experiments were carried out: the first was designed to assess the impact of monomeric versus polymer crowders by adding either monomeric EG or polymer PEG 600 to each protein system in addition to water. Each system was built from randomly placed crowders surrounding the target protein and had approximately similar numbers (~245) of monomeric EG units (Table S1). In the second experiment, the effect of the polymer's size was investigated by adding either two PEG 8K or one PEG 20k molecule in addition to water to each protein (Table S1).

3.1. Crowders' impact on backbone flexibility

The convergence of the simulation was assessed by plotting the ensemble-averaged potential energy difference along the simulation time. As demonstrated in Figure S1, the representative models comprising XPA in PEG 600 and CDKIP in PEG 8k demonstrate that the energies fluctuated less than 1 kcal/mol indicating that all protein systems converged before 20 ns.

The conformational evolution of the protein, i.e. the structural change of the backbone over time compared to the starting frame of reference was studied by plotting the evolution of RMSD along the MD simulation (Figure S2). For all protein systems, the overall conformational changes, measured by the net RMSD are listed in Table 2 and

illustrated as histograms in Figure 2. The calculated standard deviations of RMSDs were less than 1 Å, which demonstrates the equilibration of all protein systems consistent with the observed energetics (discussed above) of these simulated systems.

3.1.1. Well-folded proteins

GTPase HRas (without the highly flexible C-terminus) and pVHL, displayed reduced changes in RMSD in all crowded systems as compared to the dilute system (Figure S2a and Figure S2d). For the two well-folded proteins GTPase HRAS and pVHL (Table 2, the first and the fourth columns), the conformational space remained largely unperturbed by the crowders. The consistency of the fold, when either in an aqueous environment or surrounded by PEG crowders, suggests that these proteins tend to preserve their native conformation, which is critical for their various biological roles. In contrast, standard deviations of the RMSDs calculated using the last 10 ns of the simulation data reduced notably for all crowders (Figure 2 and Table 2). This demonstrates that for both proteins, the magnitude of conformational fluctuations was reduced in the presence of all crowders (Figure 2).

3.1.2. Partially folded proteins

Significant variations in conformational flexibilities were noted in the crowded environment for partially folded proteins XPA and CDK1P (Table 2). For these protein-crowder systems, the major structural changes occurred within the first 10 ns (Figures S2b and S2c). XPA experienced large changes in RMSD, ranging from 17 to 22 Å, in all crowded conditions, with similar changes occurring in dilute (without crowders) and crowded environments (Figure S2b). The higher-than-usual RMSDs indicate that the XPA protein underwent significant conformational changes when simulated in different crowded conditions. CDK1P also experienced large changes in RMSD, ranging from 16 to 24 Å, with the largest change occurring in the simulation with the dilute system. Thus, RMSD analysis suggests that XPA and CDK1P are both highly disordered with large conformational changes occurring in the dilute as well as in the crowded environment.

3.2. Crowders' impact on the size of protein molecules

The radius of gyration (RG) was determined for the four proteins in dilute (ie without crowders) and crowded conditions. The RG measures the distribution of mass around an object's

Table 2. Average RMSD (Å) calculated using the conformations last 10 ns of MD simulations.

Protein/crowders	GTPase HRas	XPA	CDK1P	pVHL
Dilute	4.0 (0.8)	21.4 (0.7)	23.9 (0.6)	6.3 (0.8)
EG	2.2 (0.2)	16.8 (0.7)	19.3 (0.5)	5.2 (0.3)
PEG 600	2.0 (0.1)	18.8 (0.4)	19.1 (0.4)	5.7 (0.3)
PEG 8k	2.8 (0.1)	20.8 (0.7)	18.8 (0.4)	7.6 (0.3)
PEG 20K	2.4 (0.1)	21.6 (0.5)	15.6 (0.6)	7.3 (0.2)

Notes: The standard deviations are given in parenthesis. Absolute RMSDs for all protein systems were computed using Equation (1).

center of rotation using cross sections and thus when applied to a protein system in a simulated molecular crowding environment, this measurement can provide key insight into the compactness and its change due the molecular crowding. The computed RG values were plotted over the simulated 50 ns time and shown in Figure S3 and the average values of the last 10 ns was plotted as a histogram (Figure 3). The RG remained invariant over the course of the simulation for GTPase HRas and pVHL protein systems (Figure 3). However, a decrease in the RG values over the course of the simulation was noted for partially folded XPA and CDK1P (Figures S3b-S3c). As illustrated in Figure 3, the RG values differed significantly between the dilute and crowded conditions. As these plots do not reveal any discernible pattern or correlation between polymer crowder's size and the change in RG, we investigated the interactions of crowders and these proteins.

3.3. Evidence of soft interactions between protein and crowders

The interactions between the protein and crowders were studied and the crowders' impact on the stabilization of protein was examined.

3.3.1. Interaction energy

The interaction energies with crowders plotted against the simulated time (Table 3, Figure 4) demonstrated stabilization due to protein-crowder interactions as the systems evolved.

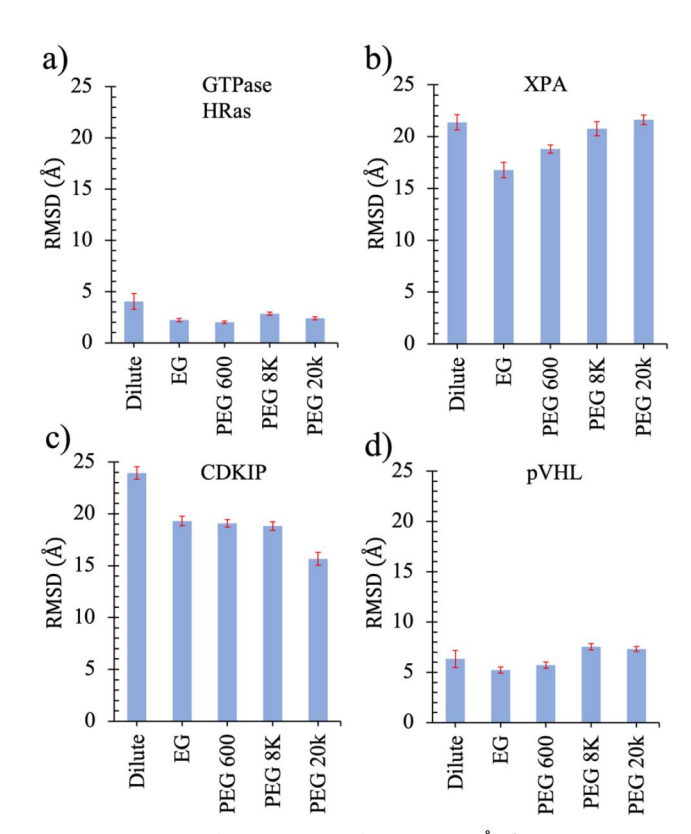


Figure 2. Histogram plots containing the RMSD (in Å) for (a) GTPase HRas, (b) XPA, (c) CDK1P and (d) pVHL. RMSDs for the backbone Ca atom were calculated using Equation (1). The average and standard deviations (shown as error bars) of the RMSDs were calculated using the last 10 ns of simulation data.

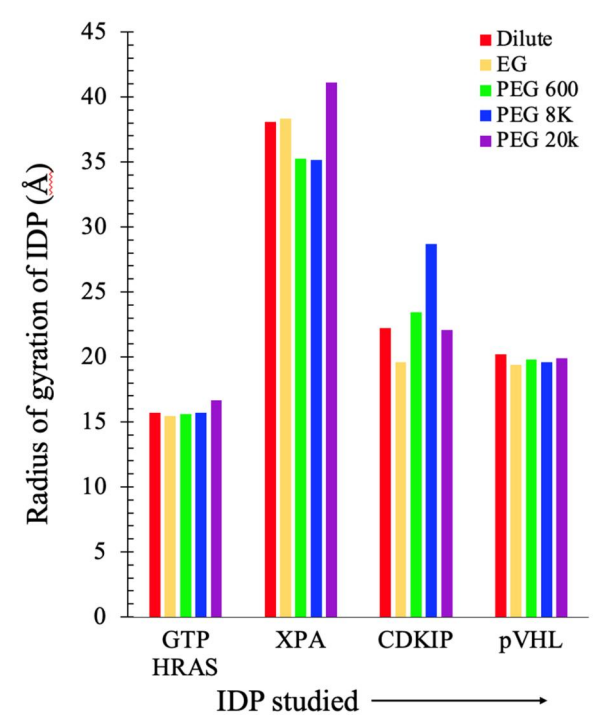


Figure 3. The radius of gyration of the four proteins averaged over the last 10 ns simulations in water, EG and PEG 600, PEG 8k and PEG 20k. The uncertainties are within 1.3 Å.

Table 3. Interaction energies (in kcal/mol) between crowders and proteins.

Protein/ crowder	GTPase HRas	XPA	CDK1P	pVHL
EG	-101.6 (26)	67.2 (42)	98.3 (33)	-64.7 (28)
PEG 600	-340.7 (38)	-393.2 (74)	-399.1 (54)	-339.8 (38)
PEG 8k	-111.5 (16)	-157.3 (21)	-48.6 (20)	-85.6 (14)
PEG 20k	-101.8 (14)	-66.6 (12)	-147.4 (15)	-112.4 (14)

Notes: The energies are the average quantities for the last 10 ns simulation. Uncertainties are given in parentheses.

For the well-folded proteins (GTPase HRas and pVHL), the interaction energy varied between -65 to $-113\,\text{kcal/mol}$ for the EG, PEG 8K and PEG 20K systems, while decreasing to \sim -340 kcal/mol for the PEG 600 system (Table 3, Figure 4(a,d)). These large negative interaction energies for PEG 600 systems (Figure 4, green lines) are indicative of enthalpic stabilization.

For the partially folded IDPs (XPA and CDKIP), the role of polymer crowders in enthalpic stabilization is more notable (Table 3). For the EG systems, the interaction energies were positive (Table 3, Figure 4(b,c), orange lines) indicating that the EG molecules tend to stay away from the protein surface. In contrast, the polymer crowders produced significantly negative interactions (Table 3) with the most negative values appearing for the PEG 600 systems. The significant enthalpic stabilization is also consistent with the visual analysis of the PEG 600 structure (Figure 5), which revealed that PEG 600 molecules tend to form aggregates (shown in Figure 5(a)) that attach to the protein surface, causing a large decrease in the enthalpy of the solvated protein-crowder system. The PEG 8k and PEG 20k shown in Figure 5(b,c) were also found to selfaggregate. Both polymers were found to wrap segments of protein surfaces, which is consistent with the variable magnitude of interaction energies: -49 to -157 kcal/mol with PEG 8k and -67 to -147 kcal/mol with PEG 20k, observed for various proteins. Thus, the above analysis provided an unambiguous interpretation of the protein-crowder soft interactions at the core of stabilizing the disordered proteins.

3.3.2. Total energy

Consistent with the large enthalpic changes due to proteincrowder interactions, the total energy in PEG 600 systems for all proteins appears to undergo a significant decrease (green

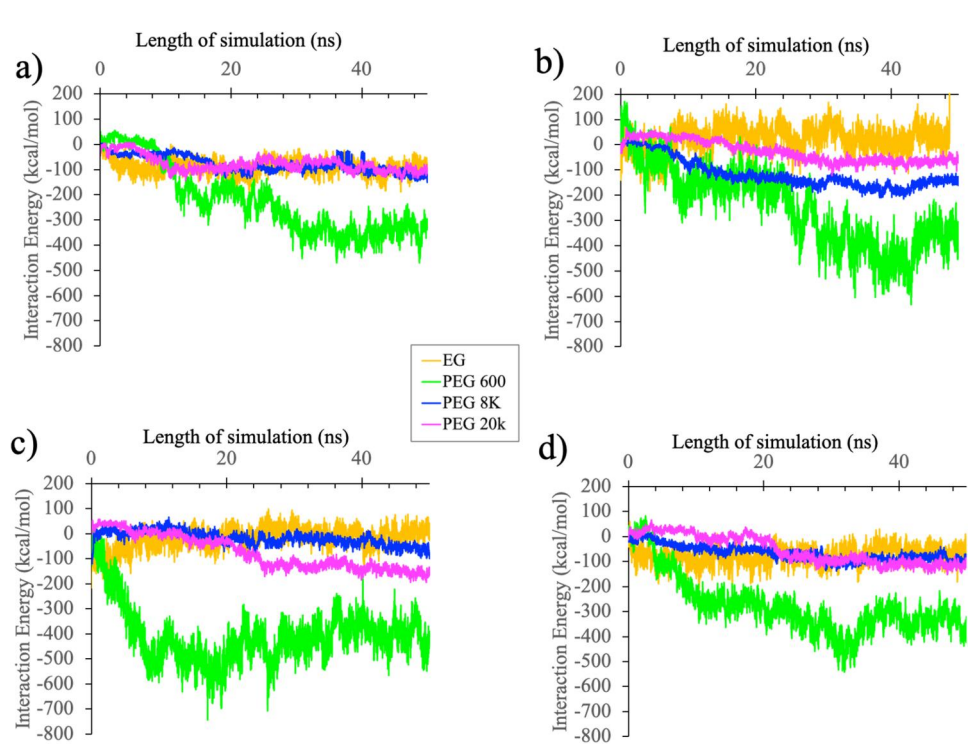


Figure 4. The change in the interaction energy between protein and crowders along the path of simulation: (a) GTPase HRas, (b) XPA, (c) CDK1P and (d) pVHL.

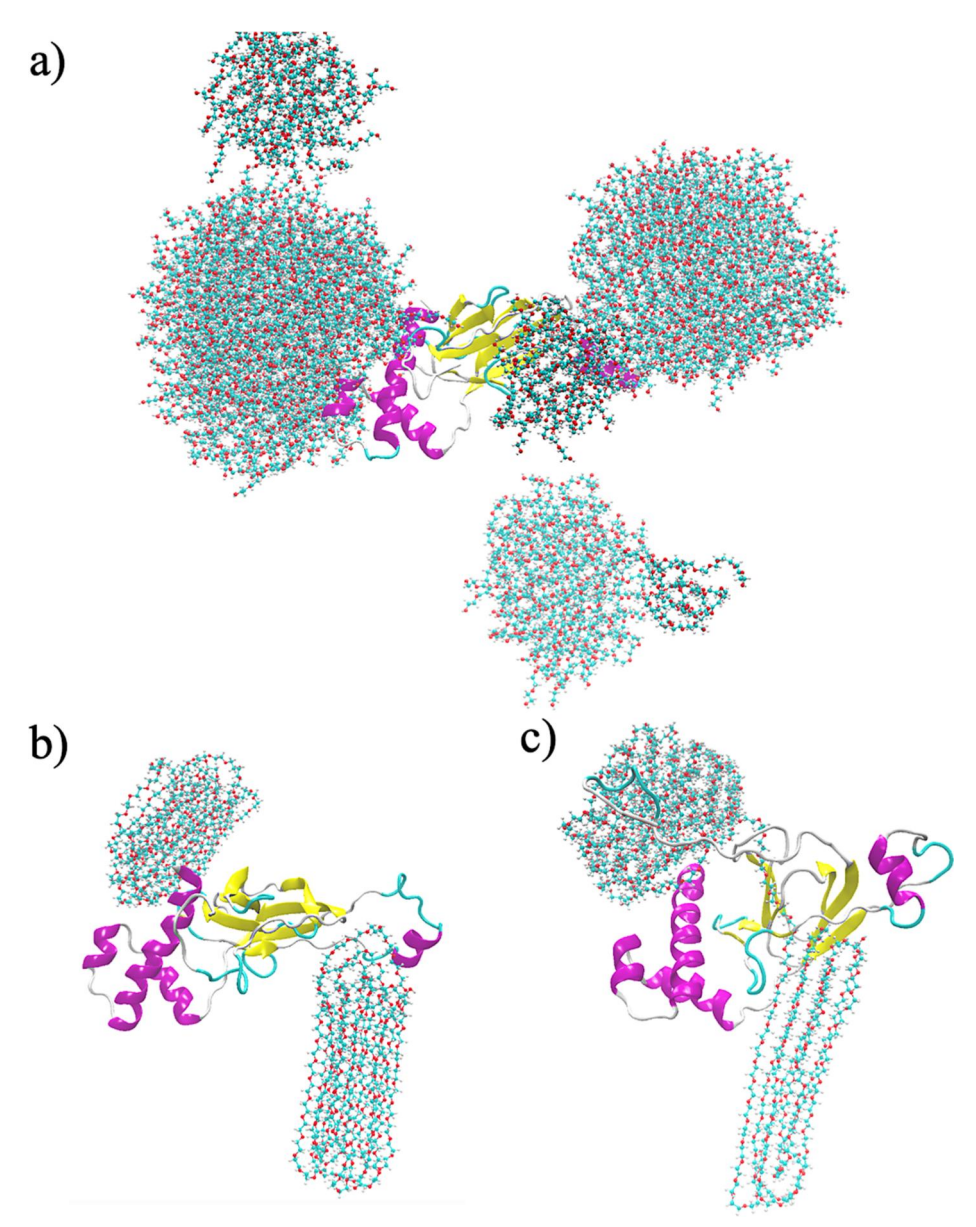


Figure 5. Visual representation of interactions between a representative protein pVHL and polymer PEG crowders: (a) PEG 600, (b) PEG 8k and (c) PEG 20k.

lines, Figure S4), compared to the dilute and EG (red and orange lines, respectively) systems. Notably, in the PEG 600-containing protein systems, a rapid decrease in energy occurred within the first 10 ns of the simulation, with a gradual decrease in the rate of change as the simulation progressed toward 50 ns. The average enthalpic change after 50 ns of simulation across all protein systems was $\sim -2300\,\text{kcal/mol}$ (Figure S4). Thus, the energetic analysis provides solid evidence of the presence of non-covalent interactions between crowder molecules as well as between crowders and proteins.

3.4. Structural alterations and disorders of proteins

As the computed RMSDs and RG along the simulation path indicates structural changes, the disorder in these proteins was also investigated by computing the conformational entropy in the presence and absence of various crowder. In

Table 4. Schlitter's entropy in kcal/(mol \times K) of the IDPs, calculated for the backbone $C\alpha$ atoms.

Protein/ crowder	GTPase HRas	XPA	CDK1P	pVHL
Dilute	1.20 ± 0.01	2.4 ± 0.1	1.58 ± 0.06	1.33 ± 0.01
EG	1.14 ± 0.02	2.37 ± 0.04	1.44 ± 0.04	1.35 ± 0.01
PEG 600	1.086 ± 0.003	2.24 ± 0.06	1.42 ± 0.02	1.27 ± 0.01
PEG 8k	1.12 ± 0.01	2.35 ± 0.05	1.39 ± 0.04	1.30 ± 0.01
PEG 20k	1.103 ± 0.006	2.4 ± 0.1	1.40 ± 0.04	1.33 ± 0.04

Note: The uncertainties are expressed in terms of the standard deviations of the entropy calculated using three sets of 10 ns data.

general, the dilute (crowder-free) did exhibit higher entropy (Table 4) than the systems simulated in the presence of polymer crowders. The PEG 600 systems across all proteins exhibited a slight decrease in entropy (Table 4). This is completely consistent with the significant stabilization observed for PEG 600 interactions with protein molecules and hence demonstrates the impact of soft interactions in lowering the disorders.

3.5. Structural alterations and disorders of the polymer crowders

Analysis of energetics revealed that maximum stabilization of proteins occurred in the presence of PEG 600 (Figure 4). The protein RMSD (Figure 2) as well as the configurational backbone entropy (Table 4) suggests that the addition of PEG 600 caused the proteins to reduce backbone fluctuations. However, our visualization indicated that the PEG 600 formed clusters of variable sizes that remained dynamic throughout the simulations. To investigate if the entropy of the crowders impacted the protein stability, the disorder of polymer chains was quantified by computing the configurational entropy and conformational changes for the three polymer crowders.

3.5.1. Configurational entropy

The configurational entropies of polymer crowders were comparable in all four protein systems indicating a consistent behavior of the crowders (Table 5). The entropies of PEG 600 were 97–99 kcal/(mol.K), which was significantly elevated compared to PEG 8k and PEG 20k, which varied 5–7 kcal/(mol.K). The increased entropy of the PEG 600 system is indicative of significant disorder.

Table 5. Schlitter's entropy in kcal/(mol \times K) for the polymer crowders.

Protein/ crowder	GTPase HRas	XPA	CDK1P	pVHL
PEG 600	99.0 ± 0.5	99.4 ± 0.4	97.6 ± 0.5	98.9 ± 0.5
PEG 8k	6.71 ± 0.09	6.60 ± 0.09	6.74 ± 0.04	6.60 ± 0.04
PEG 20k	5.13 ± 0.04	5.03 ± 0.02	5.01 ± 0.02	5.15 ± 0.02

Notes: In each case, the coordinates of only carbon atoms of the PEG backbone were taken into the calculations. The uncertainties are expressed in terms of the standard deviations of the entropy calculated using three sets of 10 ns data.

3.5.2. RMSD of conformational change

With initial positions as a reference, the RMSD changes averaged over all atoms of these polymer crowders were computed (Figure 6). The graphical representation of the RMSD changes exhibits much larger change and fluctuations in PEG 600 compared to other polymer crowders. In addition to the increase in RMSD, the plots exhibited a larger RMSD fluctuation in PEG 600 across all four protein systems. This demonstrates a larger disorder of the PEG 600 crowders, consistent to the observed entropic changes. The molecular visualization confirms that the PEG 600 molecules form dynamic clusters, which are constantly changing their sizes; a few PEG 600 molecules will dissociate from the old cluster to join a new neighboring cluster during simulations. These dynamics and disordered PEG clusters in water are therefore responsible for creating increased entropy. Therefore, it seems reasonable to conclude that the disorder of the polymer crowders themselves compensated for the entropic loss due to reduced backbone fluctuations of the disordered proteins.

3.6. Impact on dynamics and conformational ensemble

The conformational analysis examined changes in the average structure of computed conformational ensembles of each protein-crowder system using the essential dynamics analysis (Amadei et al., 1993; Tan et al., 2014). Ensembled-averaged structures representing the two main clusters of conformations in the three-dimensional principal component space (Figure 7) were determined following standard literature procedures (Glykos, 2006). For each protein-crowder system, an RMSD of the average structure was computed with respect to the ensemble-averaged structure in the

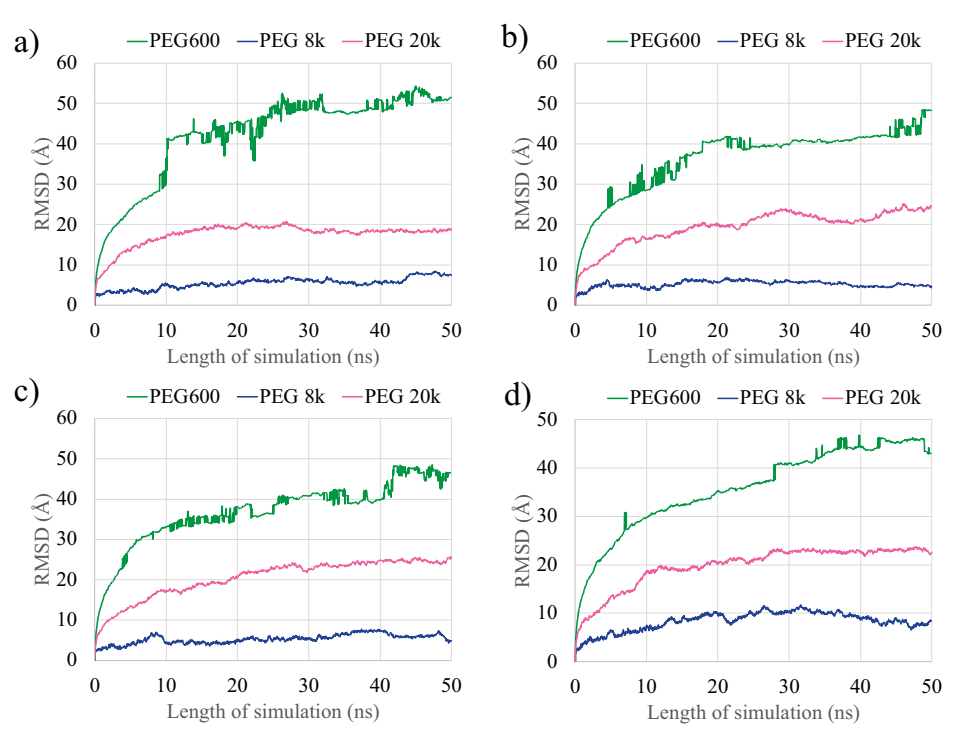


Figure 6. Plots of RMSD of PEG molecules from the initial conformation along simulation time for (a) GTPase HRas, (b) XPA, (c) CDK1P and (d) pVHL.

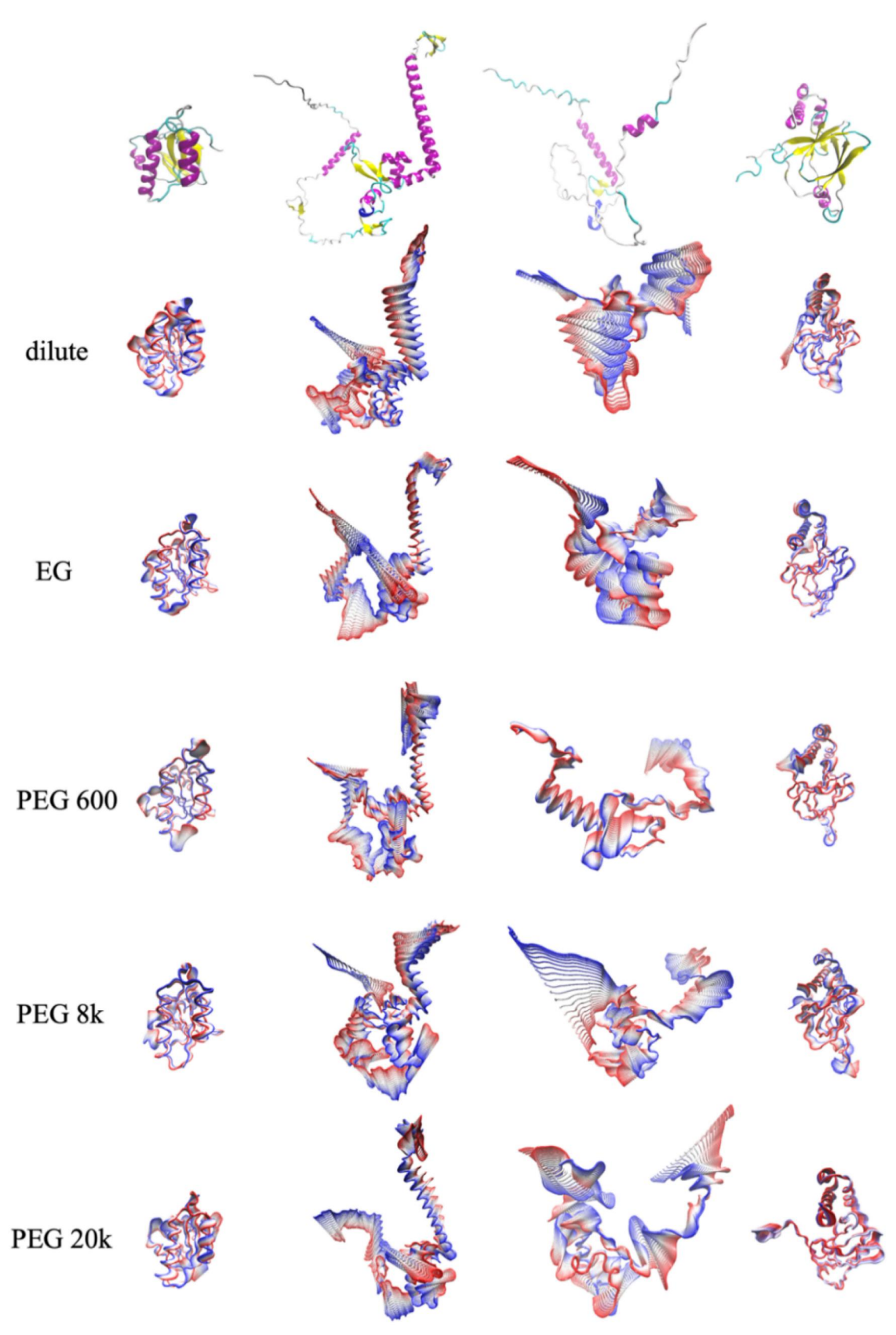


Figure 7. The major clusters identified by the first three principal components simulated in the presence of various crowders for proteins. Left to right: the GTPase HRas, XPA, CDK1P and pVHL. The top panel illustrates the alpha-fold structures. The red-to-blue colors are representative of the conformational span with the beginning and ending structures, respectively, during the course of 50 ns simulations.

dilute (ie crowder-free) state (Table 6). The percentage of conformations obtained in these PCA-derived ensembles is shown in parentheses. For each protein system, the average structures of the main cluster of conformations differ across the crowders, and the pair-wise calculated RMDSs are given in Table S2.

Table 6. Conformational change of proteins in the presence of various crowders.

	Clusters	Dilute	EG	PEG 600	PEG 8k	PEG 20K
GTPase HRas	First	0.00 (65)	3.37 (12)	3.40 (24)	3.79 (34)	1.99 (21)
	Second	0.00 (9)	3.27 (13)	3.05 (12)	3.46 (15)	2.84 (20)
XPA	First	0.00 (33)	21.77 (13)	22.64 (42)	15.95 (58)	20.95 (56)
	Second	0.00 (8)	14.68 (17)	17.07 (6)	18.72 (8)	20.50 (19)
CDK1P	First	0.00 (17)	18.96 (40)	19.98 (41)	14.96 (30)	15.44 (49)
	Second	0.00 (26)	17.38 (7)	18.22 (30)	23.41 (20)	21.33 (11)
pVHL	First	0.00 (20)	3.76 (50)	3.86 (24)	3.86 (36)	7.61 (58)
	Second	0.00 (8)	-	7.26 (54)	5.88 (24)	-

Notes: The conformational change is measured as RMSD (in Å) between the average structure of conformational ensembles, obtained for the two densely populated clusters in the three-dimensional principal component space during essential dynamics analysis. The percentage of populations is given in parentheses. For each protein, the conformation of the average structure obtained from the highest populated cluster in dilute condition was taken as a reference.

3.6.1. GTPase HRas and pVHL

The PCA-derived cluster analysis (Table 6) of GTPase HRas demonstrated revealed only minor changes in the RMSD across all crowded systems compared to the dilute system (Figure 7, the left-most columns). In particular, the RMSD values for GTPase HRas ranged from 2.0 to 3.8 Å, with the largest deviation occurring in the presence of the PEG 8k crowder (Table 6). A pair-wise analysis of these cluster-averaged structures (Table S2) across various crowders exhibited that the RMSD changed by only 1.6 to 2.8 Å confirming the conformational rigidity of the protein in crowded conditions.

The population analysis (in %) revealed that GTPase HRas conformations were redistributed between the two main clusters (Table 6, in parentheses) as crowder conditions changed. This suggests that although conformational changes were marginal, the crowders altered the distribution of conformations in the two ensembles in GTPase HRas.

Like GTPase HRas, pVHL underwent minimal structural changes in the ensemble of structures (Figure 7, the rightmost column). This is also evident from the RMSD of the representative structure of the largest cluster of conformations in the dilute structure taken as a reference structure. Notably, PEG 20k induced the largest conformational shift in the pVHL system, at 7.61 Å. A pair-wise analysis of these cluster-averaged structures (Table S2) exhibited a larger variation, 3.8 to 7.6 Å, which suggests relatively more crowder-induced conformational flexibility than GTPase HRas. A significant change in the conformational distribution was noted for this protein. For the EG and PEG 20k systems, there was a single predominant cluster, while for PEG 600, the second cluster was significantly more populated (54%) than the first one (24%). This indicates that the conformational distribution was certainly impacted by the type of crowders.

3.6.2. XPA and CDK1P

In the XPA-containing systems the structural changes are significant as indicated by the large span of the backbone (Figure 7, second from the left). The computed RMSDs ranged from 14.68–22.64 Å in crowded conditions compared to the dilute references (Table 6) confirming that the

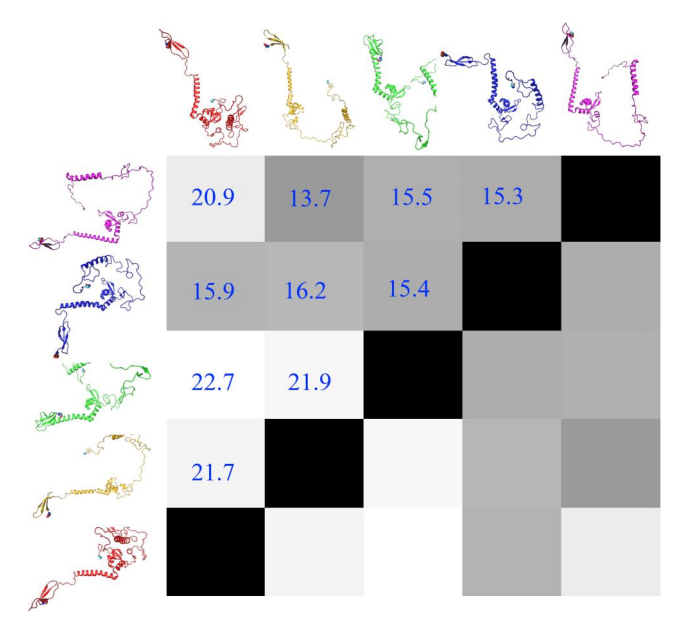


Figure 8. Significant conformational dynamism was observed for the proteins using essential dynamics and cluster analysis. The significantly disordered protein XPA was taken as a representative model. The structural differences between the average structures obtained from the densest cluster of conformations are presented as a 2D matrix. The structures shown are color-coded with red (dilute), orange (EG), green (PEG 600), blue (PEG 8k) and purple (PEG 20k). The matrix is symmetric with the off-diagonal elements in gray colormap labeled with backbone RMSD values between two conformations. The black indicates a 0 Å RMSD occurring between the same protein conformation.

crowder impacted conformational diversity. A pair-wise structural analysis of the first major cluster of conformations was carried out (Table S2), which confirm that these crowder-induced clusters of conformations are significantly different from each other. As a representative comparative study, Figure 8 displays the diversity of these structures of XPA across all crowders by computing the RMSDs. The distribution of population in the major cluster of conformations was also significantly different in different environments (Table 6).

Large conformational variation, similar to XPA, was also observed for the PCA-derived major cluster of CDK1P (Figure 7, third column from the left). The ensemble-average structures exhibited relatively large changes in RMSD ranging from 15 to 23 Å (Table 6), as compared to the structure observed in the dilute system. The pair-wise structure comparison (Table S2) reinforces the idea that the molecular crowders significantly impacted conformational diversity. The population distribution differed as well (Table 6, in parentheses). The analysis shows that for the partially folded proteins, the crowders not only altered the conformational space significantly but also its distribution across different conformational ensembles.

In summary, the results of the two experiments portray the enthalpic and entropic contributions of the molecular crowders in the stabilization of disordered proteins. The first experiment demonstrates that for polymer crowders the enthalpic (crowder-protein interactions) as well as entropic (disorders in crowders) effects are significantly stronger than their monomer and crowder-free (dilute) states. The second experiment reveals that the enthalpic and entropic effects do not depend on the chain length of the PEG polymers.



4. Conclusions

Protein dynamics are dependent on the type of crowders. The present study provides insight into how crowders impact the well-folded and partially folded proteins (Figure 1, Table 1). Four proteins of similar size were studied using a 50 ns MD simulation. The structural changes indicated the extent of folding; RMSDs of the well-folded GTPase HRas and pVHL were less than 8 Å. In contrast, the RMSDs of partially folded XPA and CDKIP were recorded to reach as high as 25 Å (Figure 2, Table 2). The analysis of simulated structures found that the partially folded proteins shrunk in size as evidenced by the decrease in their radius of gyration (Figure S3).

The study found that the stability of IDPs was contributed by enthalpic as well as entropic changes. The computed protein-crowders interaction energies demonstrate that monomer crowders tend to destabilize the partially folded proteins while stabilizing the well-folded proteins (Table 3). The interaction energy is significantly negative for polymer crowders indicating enthalpic stabilization through soft interactions. The largest stabilization energy occurred for PEG 600 (Table 3). Our study also confirms that the interactions reduced the disorder of the protein backbone. Schlitter's entropy calculations exhibited a consistent pattern of decreasing disorder of the protein backbone, with the largest decrease occurring for PEG 600 (Figure 4, Table 4). This demonstrates the existence of soft interaction between protein and polymer crowders, which was confirmed visually (Figure 5).

The essential dynamics analysis revealed that for GTPase HRas and pVHL, the two well-folded proteins, the crowded environments caused little change in the conformational space observed through three major principal component dimensions (Figure 7, left and right columns). Due to their folded structure, these proteins have segments with limited conformational flexibility, which exhibited little or no change due to the presence of crowders. This is established by the smaller values of RMSDs, generated by PCA-derived clusters in crowders when measured with respect to their dilute state backbone structure (Table 6). The population analysis however exhibited a significant difference in the major conformation ensembles. Therefore, crowder-induced dynamics appear to contribute to the disorder through a conformational redistribution.

In contrast, for the partially folded protein systems, XPA and CDK1P, the top clusters show significant RMSD differences (Table 6) indicating large conformational changes in the predominant cluster of conformations. Interestingly, the disorder decreases noticeably when surrounded by polymer crowders (Figure 7, the two central columns) compared to what was observed in the dilute condition, especially for PEG 600. Additionally, the simulated models exhibited that these crowders led to a significant change in the conformational distribution of these IDPs as well, when compared with various crowded surroundings.

Taken together, the MD simulation study using two distinct experiments demonstrated that polymer crowders have a higher impact in restricting the conformational space of the disordered proteins compared to the monomer and crowder-free states. However, increasing the chain length did not produce a different outcome. Under various crowded states, these partially folded proteins can adopt a significantly diverse ensemble of conformational states (Figure 8), which is indicative of their ability to generate dynamic scaffolds needed to carry out diverse functions. Although the current study is limited in observing the effect of various crowders on the structural transition, the theoretical models can be used as a prototype to further probe the structurefunction relationships of these IDPs.

Acknowledgments

The authors thank the supercomputing resources available at the Blugold Center for High-Performance Computing of the University of Wisconsin-Eau Claire.

Author contributions

C.S., K.G., S.J.C., B.M., M.B., L.S., J.S., E.R.O., S.E.S. and N.J.S. were involved in carrying out the computational experiments, data curation, analysis, interpretation and writing up the results. C.S. compiled results and drafted the manuscript. K.G., S.H. and S.B. revised it critically for intellectual content. S.H. and S.B. conceptualized the study, designed experiments, supervised and edited the manuscript. All authors approve the final version to be published and agree to be accountable for all aspects of the work.

Disclosure statement

No potential conflict of interest was reported by the authors.

Funding

This work was supported, in part, by the National Institute of Health (grant number: 2R15GM117510-02 to S.H. and S.B.) and the Office of Research and Sponsored Program of the University of Wisconsin-Eau Claire. The computational resources were funded under NSF grant CNS 1920220.

ORCID

Sanchita Hati http://orcid.org/0000-0002-7452-0872 Sudeep Bhattacharyay (D) http://orcid.org/0000-0002-3960-1239

Data availability statement

The datasets generated during and/or analyzed during the current study are available from the corresponding author upon reasonable request.

References

Al Bitar, S., & Gali-Muhtasib, H. (2019). The role of the cyclin dependent kinase inhibitor p21cip1/waf1 in targeting cancer: Molecular mechanisms and novel therapeutics. Cancers, 11(10), 1475. https://doi.org/ 10.3390/cancers11101475

Amadei, A., Linssen, A. B., & Berendsen, H. J. (1993). Essential dynamics of proteins. Proteins, 17(4), 412-425. https://doi.org/10.1002/prot. 340170408

Berrada, N., Amzazi, S., Abbar, M., Ameur, A., Khyatti, M., Al-Bouzidi, A., & Attaleb, M. (2015). Mutational analysis of FGFR3 and HRAS genes in bladder cancer and washing cell sediments of Moroccan patients.



- Epidemiology (sunnyvale), 5, 214. https://doi.org/10.4172/2167-0277.
- Bertoli, C., Skotheim, J. M., & De Bruin, R. A. M. (2013). Control of cell cycle transcription during G1 and S phases. Nature Reviews. Molecular Cell Biology, 14(8), 518-528. https://doi.org/10.1038/nrm3629
- Bertoline, L. M. F., Lima, A. N., Krieger, J. E., & Teixeira, S. K. (2023). Before and after AlphaFold2: An overview of protein structure prediction. Frontiers in Bioinformatics, 3, 1120370. https://doi.org/10.3389/ fbinf.2023.1120370
- Bondos, S. E., Dunker, A. K., & Uversky, V. N. (2022). Intrinsically disordered proteins play diverse roles in cell signaling. Cell Communication and Signaling: CCS, 20(1), 20. https://doi.org/10.1186/s12964-022-00821-7
- Bonucci, A., Palomino-Schätzlein, M., Malo de Molina, P., Arbe, A., Pierattelli, R., Rizzuti, B., Iovanna, J. L., & Neira, J. L. (2021). Crowding effects on the structure and dynamics of the intrinsically disordered nuclear chromatin protein NUPR1. Frontiers in Molecular Biosciences, 8, 684622. https://doi.org/10.3389/fmolb.2021.684622
- Bradford, P. T., Goldstein, A. M., Tamura, D., Khan, S. G., Ueda, T., Boyle, J., Oh, K. S., Imoto, K., Inui, H., Moriwaki, S. I., Emmert, S., Pike, K. M., Raziuddin, A., Plona, T. M., DiGiovanna, J. J., Tucker, M. A., & Kraemer, K. H. (2011). Cancer and neurologic degeneration in xeroderma pigmentosum: Long term follow-up characterises the role of DNA repair. Journal of Medical Genetics, 48(3), 168-176. https://doi.org/10.1136/ jmg.2010.083022
- Brooks, B. R., Bruccoleri, R. E., Olafson, B. D., States, D. J., Swaminathan, S. J., & Karplus, M. (1983). CHARMM: A program for macromolecular energy, minimization, and dynamics calculations. Journal of Computational Chemistry, 4(2), 187-217. https://doi.org/10.1002/jcc.540040211
- Cheatham, T. E., Miller, J. L., Fox, T., Darden, T. A., & Kollman, P. A. (1995). Molecular dynamics simulations on solvated biomolecular systems: The particle mesh Ewald method leads to stable trajectories of DNA, RNA, and proteins, Journal of the American Chemical Society, 117(14), 4193-4194. https://doi.org/10.1021/ja00119a045
- Cheung, M. S., Klimov, D., & Thirumalai, D. (2005). Molecular crowding enhances native state stability and refolding rates of globular proteins. Proceedings of the National Academy of Sciences of the United States of America, 102(13), 4753-4758. https://doi.org/10.1073/pnas. 0409630102
- Cho, E. J., & Kim, J. S. (2012). Crowding effects on the formation and maintenance of nuclear bodies: Insights from molecular-dynamics simulations of simple spherical model particles. Biophysical Journal, 103(3), 424-433. https://doi.org/10.1016/j.bpj.2012.07.007
- Chong, S. H., Chatterjee, P., & Ham, S. (2017). Computer simulations of intrinsically disordered proteins. Annual Review of Physical Chemistry, 68(1), 117-134. https://doi.org/10.1146/annurev-physchem-052516-050843
- Deng, C., Zhang, P., Harper, J. W., Elledge, S. J., & Leder, P. (1995). Mice lacking p21 CIP1/WAF1 undergo normal development, but are defective in G1 checkpoint control. Cell, 82(4), 675-684. https://doi.org/10. 1016/0092-8674(95)90039-X
- Dignon, G. L., Zheng, W., Kim, Y. C., & Mittal, J. (2019). Temperature-controlled liquid-liquid phase separation of disordered proteins. ACS Central Science, 5(5), 821-830. https://doi.org/10.1021/acscentsci. 9b00102
- Dill, K. A., Ozkan, S. B., Scott Shell, M., & Weikl, T. R. (2008). The protein folding problem. Annual Review of Biophysics, 37(1), 289-316. https:// doi.org/10.1146/annurev.biophys.37.092707.153558
- Dunker, A. K., Brown, C. J., Lawson, J. D., Iakoucheva, L. M., & Obradović, Z. (2002). Intrinsic disorder and protein function. Biochemistry, 41(21), 6573–6582. https://doi.org/10.1021/bi012159+
- Dyson, H. J., & Wright, P. E. (2004). Unfolded proteins and protein folding studied by NMR. Chemical Reviews, 104(8), 3607-3622. https://doi.org/ 10.1021/cr030403s
- Dyson, H. J., & Wright, P. E. (2005). Intrinsically unstructured proteins and their functions. Nature Reviews. Molecular Cell Biology, 6(3), 197–208. https://doi.org/10.1038/nrm1589
- Dzuricky, M., Rogers, B. A., Shahid, A., Cremer, P. S., & Chilkoti, A. (2020). De novo engineering of intracellular condensates using artificial disordered proteins. Nature Chemistry, 12(9), 814-825. https://doi.org/10. 1038/s41557-020-0511-7

- Essmann, U., Perera, L., Berkowitz, M. L., Darden, T., Lee, H., & Pedersen, L. G. (1995). A smooth particle mesh Ewald method. The Journal of Chemical Physics, 103(19), 8577-8593. https://doi.org/10.1063/1.470117
- Evans, R., Ramisetty, S., Kulkarni, P., & Weninger, K. (2023). Illuminating intrinsically disordered proteins with integrative structural biology. Biomolecules, 13(1), 124. https://doi.org/10.3390/biom13010124
- Fagerberg, E., Lenton, S., & Skepö, M. (2019). Evaluating models of varying complexity of crowded intrinsically disordered protein solutions against SAXS. Journal of Chemical Theory and Computation, 15(12), 6968-6983. https://doi.org/10.1021/acs.jctc.9b00723
- Feller, S. E., Zhang, Y., Pastor, R. W., & Brooks, B. R. (1995). Constant pressure molecular dynamics simulation: The Langevin piston method. The Journal of Chemical Physics, 103(11), 4613-4621. https://doi.org/ 10.1063/1.470648
- Felli, I. C., & Pierattelli, R. (2012). Recent progress in NMR spectroscopy: Toward the study of intrinsically disordered proteins of increasing size and complexity. IUBMB Life, 64(6), 473-481. https://doi.org/10.1002/ iub.1045
- Fonin, A. V., Darling, A. L., Kuznetsova, I. M., Turoverov, K. K., & Uversky, V. N. (2018). Intrinsically disordered proteins in crowded milieu: When chaos prevails within the cellular gumbo. Cellular and Molecular Life Sciences: CMLS, 75(21), 3907-3929. https://doi.org/10.1007/s00018-018-2894-9
- García-Carmona, J. A., Yousefzadeh, M. J., Alarcón-Soldevilla, F., Fages-Caravaca, E., Kieu, T. L., Witt, M. A., López-Ávila, Á., Niedernhofer, L. J., & Pérez-Vicente, J. A. (2021). Case report: Identification of a heterozygous XPA c.553C > T mutation causing neurological impairment in a case of xeroderma pigmentosum complementation group A. Frontiers in Genetics, 12, 717361. https://doi.org/10.3389/fgene.2021.717361
- Garcia-Rostan, G., Zhao, H., Camp, R. L., Pollan, M., Herrero, A., Pardo, J., Wu, R., Carcangiu, M. L., Costa, J., & Tallini, G. (2003). ras Mutations are associated with aggressive tumor phenotypes and poor prognosis in thyroid cancer. Journal of Clinical Oncology, 21(17), 3226-3235. https://doi.org/10.1200/JCO.2003.10.130
- Gething, M. J., & Sambrook, J. (1992). Protein folding in the cell. Nature, 355(6355), 33-45. https://doi.org/10.1038/355033a0
- Glykos, N. M. (2006). Software news and updates. Carma: A molecular dynamics analysis program. Journal of Computational Chemistry, 27(14), 1765-1768. https://doi.org/10.1002/jcc.20482
- Huang, J., & Mackerell, A. D. (2013). CHARMM36 all-atom additive protein force field: Validation based on comparison to NMR data. Journal of Computational Chemistry, 34(25), 2135-2145. https://doi.org/10.1002/ icc.23354
- Humphrey, W., Dalke, A., & Schulten, K. (1996). VMD: Visual molecular dynamics. Journal of Molecular Graphics, 14(1), 33-38. https://doi.org/ 10.1016/0263-7855(96)00018-5
- Igarashi, H., Esumi, M., Ishida, H., & Okada, K. (2002). Vascular endothelial growth factor overexpression is correlated with von Hippel-Lindau tumor suppressor gene inactivation in patients with sporadic renal cell carcinoma. Cancer, 95(1), 47-53. https://doi.org/10.1002/cncr.10635
- Jorgensen, W. L., Chandrasekhar, J., Madura, J. D., Impey, R. W., & Klein, M. L. (1983). Comparison of simple potential functions for simulating liquid water. The Journal of Chemical Physics, 79(2), 926-935. https:// doi.org/10.1063/1.445869
- Jumper, J., Evans, R., Pritzel, A., Green, T., Figurnov, M., Ronneberger, O., Tunyasuvunakool, K., Bates, R., Žídek, A., Potapenko, A., Bridgland, A., Meyer, C., Kohl, S. A. A., Ballard, A. J., Cowie, A., Romera-Paredes, B., Nikolov, S., Jain, R., Adler, J., ... Hassabis, D. (2021). Highly accurate protein structure prediction with AlphaFold. Nature, 596(7873), 583-589. https://doi.org/10.1038/s41586-021-03819-2
- Kaelin, W. G. (2002). Molecular basis of the VHL hereditary cancer syndrome. Nature Reviews. Cancer, 2(9), 673-682. https://doi.org/10.1038/nrc885
- Kaelin, W. G. (2007). The von Hippel-Lindau tumor suppressor protein and clear cell renal carcinoma. Clinical Cancer Research, 13(2 Pt 2), 680s-684s. https://doi.org/10.1158/1078-0432.CCR-06-1865
- Kikhney, A. G., & Svergun, D. I. (2015). A practical guide to small angle X-ray scattering (SAXS) of flexible and intrinsically disordered proteins. FEBS Letters, 589(19 Pt A), 2570-2577. https://doi.org/10.1016/j.febslet. 2015.08.027



- Kim, W. Y., & Kaelin, W. G. (2004). Role of VHL gene mutation in human cancer. Journal of Clinical Oncology, 22(24), 4991-5004. https://doi. org/10.1200/JCO.2004.05.061
- Kosol, S., Contreras-Martos, S., Cedeño, C., & Tompa, P. (2013). Structural characterization of intrinsically disordered proteins by NMR spectroscopy. Molecules, 18(9), 10802-10828. https://doi.org/10.3390/molecules 180910802
- Kriwacki, R. W., Hengst, L., Tennant, L., Reed, S. I., & Wright, P. E. (1996). Structural studies of p21Waf1/Cip1/Sdi1 in the free and Cdk2-bound state: Conformational disorder mediates binding diversity. Proceedings of the National Academy of Sciences of the United States of America, 93(21), 11504-11509. https://doi.org/10.1073/pnas.93.21.11504
- Laatsch, B. F., Brandt, M., Finke, B., Fossum, C. J., Wackett, M. J., Lowater, H. R., Narkiewicz-Jodko, A., Le, C. N., Yang, T., Glogowski, E. M., Bailey-Hartsel, S. C., Bhattacharyya, S., & Hati, S. (2023). Polyethylene glycol 20k. Does it fluoresce? ACS Omega, 8(15), 14208-14218. https://doi. org/10.1021/acsomega.3c01124
- Li, B., Fooksa, M., Heinze, S., & Meiler, J. (2018). Finding the needle in the haystack: Towards solving the protein-folding problem computationally. Critical Reviews in Biochemistry and Molecular Biology, 53(1), 1-28. https://doi.org/10.1080/10409238.2017.1380596
- Lin, Y. H., & Chan, H. S. (2017). Phase separation and single-chain compactness of charged disordered proteins are strongly correlated. Biophysical Journal, 112(10), 2043-2046. https://doi.org/10.1016/j.bpj.2017.04.021
- Malumbres, M., & Barbacid, M. (2003). RAS oncogenes: The first 30 years. Nature Reviews. Cancer, 3(6), 459-465. https://doi.org/10.1038/nrc1097
- Menon, S., & Mondal, J. (2023). Conformational plasticity in α-synuclein and how crowded environment modulates it. The Journal of Physical Chemistry B, 127(18), 4032-4049. https://doi.org/10.1021/acs.jpcb.3c00982
- Morris, O. M., Torpey, J. H., & Isaacson, R. L. (2021). Intrinsically disordered proteins: Modes of binding with emphasis on disordered domains. Open Biology, 11(10), 210222. https://doi.org/10.1098/rsob.210222
- Munishkina, L. A., Ahmad, A., Fink, A. L., & Uversky, V. N. (2008). Guiding protein aggregation with macromolecular crowding. Biochemistry, 47(34), 8993-9006. https://doi.org/10.1021/bi8008399
- Na, J. H., Lee, W. K., & Yu, Y. G. (2018). How do we study the dynamic structure of unstructured proteins: A case study on nopp140 as an example of a large, intrinsically disordered protein. International Journal of Molecular Sciences, 19(2), 381. https://doi.org/10.3390/ijms19020381
- Nikiforov, Y. E., & Nikiforova, M. N. (2011). Molecular genetics and diagnosis of thyroid cancer. Nature Reviews. Endocrinology, 7(10), 569-580. https://doi.org/10.1038/nrendo.2011.142
- Ohh, M., Taber, C. C., Ferens, F. G., & Tarade, D. (2022). Hypoxia-inducible factor underlies von Hippel-Lindau disease stigmata. eLife, 11, e80774. https://doi.org/10.7554/eLife.80774
- Phillips, J. C., Braun, R., Wang, W., Gumbart, J., Tajkhorshid, E., Villa, E., Chipot, C., Skeel, R. D., Kalé, L., & Schulten, K. (2005). Scalable molecular dynamics with NAMD. Journal of Computational Chemistry, 26(16), 1781-1802. https://doi.org/10.1002/jcc.20289
- Phillips, J. C., Hardy, D. J., Maia, J. D. C., Stone, J. E., Ribeiro, J. V., Bernardi, R. C., Buch, R., Fiorin, G., Hénin, J., Jiang, W., McGreevy, R., Melo, M. C. R., Radak, B. K., Skeel, R. D., Singharoy, A., Wang, Y., Roux, B., Aksimentiev, A., Luthey-Schulten, Z., ... Tajkhorshid, E. (2020). Scalable molecular dynamics on CPU and GPU architectures with NAMD. The Journal of Chemical Physics, 153(4), 044130. https://doi.org/10.1063/5.0014475
- Putnam, C. D., Hammel, M., Hura, G. L., & Tainer, J. A. (2007). X-ray solution scattering (SAXS) combined with crystallography and computation: Defining accurate macromolecular structures, conformations and assemblies in solution. Quarterly Reviews of Biophysics, 40(3), 191-285. https://doi.org/10.1017/S0033583507004635
- Qi, H. W., Nakka, P., Chen, C., & Radhakrishnan, M. L. (2014). The effect of macromolecular crowding on the electrostatic component of Barnase-Barstar binding: A computational, implicit solvent-based study. PLoS One, 9(6), e98618. https://doi.org/10.1371/journal.pone.0098618
- Quiroz, F. G., Li, N. K., Roberts, S., Weber, P., Dzuricky, M., Weitzhandler, I., Yingling, Y. G., & Chilkoti, A. (2019). Intrinsically disordered proteins access a range of hysteretic phase separation behaviors. Science Advances, 5(10), eaax5177. https://doi.org/10.1126/sciadv.aax5177
- Rademakers, S., Volker, M., Hoogstraten, D., Nigg, A. L., Moné, M. J., van Zeeland, A. A., Hoeijmakers, J. H. J., Houtsmuller, A. B., & Vermeulen, W. (2003). Xeroderma pigmentosum group A protein loads as a

- separate factor onto DNA lesions. Molecular and Cellular Biology, 23(16), 5755-5767. https://doi.org/10.1128/MCB.23.16.5755-5767.2003
- Receveur-Brechot, V., & Durand, D. (2012). How random are intrinsically disordered proteins? A small angle scattering perspective. Current Protein & Peptide Science, 13(1), 55-75. https://doi.org/10.2174/ 138920312799277901
- Rehman, I., Kerndt, C. C., & Botelho, S. (2022). Biochemistry, tertiary protein structure. In StatPearls (Ed.), StatPearls [Internet]. StatPearls.
- Sarkar, A., Gasic, A. G., Cheung, M. S., & Morrison, G. (2022). Effects of protein crowders and charge on the folding of superoxide dismutase 1 variants: A computational study. The Journal of Physical Chemistry. B, 126(24), 4458–4471. https://doi.org/10.1021/acs.jpcb.2c00819
- Schlitter, J. (1993). Estimation of absolute and relative entropies of macromolecules using the covariance matrix. Chemical Physics Letters, 215(6), 617-621. https://doi.org/10.1016/0009-2614(93)89366-P
- Soranno, A., Koenig, I., Borgia, M. B., Hofmann, H., Zosel, F., Nettels, D., & Schuler, B. (2014). Single-molecule spectroscopy reveals polymer effects of disordered proteins in crowded environments. Proceedings of the National Academy of Sciences of the United States of America, 111(13), 4874-4879. https://doi.org/10.1073/pnas.1322611111
- Straiton, J. (2023). The path to solving the protein folding problem. BioTechniques, 74(5), 199-201. https://doi.org/10.2144/btn-2023-0031
- Sugasawa, K., Ng, J. M. Y., Masutani, C., Iwai, S., Van Der Spek, P. J., Eker, A. P. M., Hanaoka, F., Bootsma, D., & Hoeijmakers, J. H. J. (1998). Xeroderma pigmentosum group C protein complex is the initiator of global genome nucleotide excision repair. Molecular Cell, 2(2), 223-232. https://doi.org/10.1016/S1097-2765(00)80132-X
- Tan, Y., Hanson, J. A., Chu, J., & Yang, H. (2014). Principal component analysis: A method for determining the essential dynamics of proteins. Proteins, 1084, 51-62. https://doi.org/10.1007/978-1-62703-658-0
- Uversky, V. N. (2009). Intrinsically disordered proteins and their environment: Effects of strong denaturants, temperature, pH, counter ions, membranes, binding partners, osmolytes, and macromolecular crowding. The Protein Journal, 28(7-8), 305-325. https://doi.org/10.1007/s10930-009-9201-4
- Uversky, V. N. (2019). Intrinsically disordered proteins and their "mysterious" (meta)physics. Frontiers in Physics, 7(10), 1-18. https:// doi.org/10.3389/fphy.2019.00010
- Vageli, D., Kiaris, H., Delakas, D., Anezinis, P., Cranidis, A., & Spandidos, D. A. (1996). Transcriptional activation of H-ras, K-ras and N-ras protooncogenes in human bladder tumors. Cancer Letters, 107(2), 241-247. https://doi.org/10.1016/0304-3835(96)04372-8
- Varadi, M., Anyango, S., Deshpande, M., Nair, S., Natassia, C., Yordanova, G., Yuan, D., Stroe, O., Wood, G., Laydon, A., Žídek, A., Green, T., Tunyasuvunakool, K., Petersen, S., Jumper, J., Clancy, E., Green, R., Vora, A., Lutfi, M., ... Velankar, S. (2022). AlphaFold Protein Structure Database: Massively expanding the structural coverage of proteinsequence space with high-accuracy models. Nucleic Acids Research, 50(D1), D439-D444. https://doi.org/10.1093/nar/gkab1061
- Verlet, L. (1967). Computer "experiments" on classical fluids. I. Thermodynamical properties of Lennard-Jones molecules. Physical Review, 159(1), 98-103. https://doi.org/10.1103/PhysRev.159.98
- Vries, A. D., Van Oostrom, C. T. M., Hofhuis, F. M. A., Dortant, P. M., Berg, R. J. W., Gruijl, F. R. D., Wester, P. W., Van Kreijl, C. F., Capel, P. J. A., Steeg, H. V., & Verbeek, S. J. (1995). Increased susceptibility to ultraviolet-B and carcinogens of mice lacking the DNA excision repair gene XPA. Nature, 377(6545), 169-173. https://doi.org/10.1038/377169a0
- Wright, P. E., & Dyson, H. J. (1999). Intrinsically unstructured proteins: Re-assessing the protein structure-function paradigm. Journal of Molecular Biology, 293(2), 321-331. https://doi.org/10.1006/jmbi.1999.3110
- Zhou, H. X. (2008). Protein folding in confined and crowded environments. Archives of Biochemistry and Biophysics, 469(1), 76-82. https:// doi.org/10.1016/j.abb.2007.07.013
- Zhou, H. X., Rivas, G., & Minton, A. P. (2008). Macromolecular crowding and confinement: Biochemical, biophysical, and potential physiological consequences. Annual Review of Biophysics, 37(1), 375-397. https://doi.org/10.1146/annurev.biophys.37.032807.125817
- Zimmerman, S. B., & Minton, A. P. (1993). Macromolecular crowding: Biochemical, biophysical, and physiological consequences. Annual Review of Biophysics and Biomolecular Structure, 22(1), 27-65. https:// doi.org/10.1146/annurev.bb.22.060193.000331